www.jcimcr.org

JCIMCR OPEN ACCESS Journal of Clinical Images and Medical Case Reports

ISSN 2766-7820

Research Article

Open Access, Volume 5

Neural networks-based damage detection for symmetrical structures considering modal feature similarity

Renling Zou[1]*; Jiaqing Wang[1]; Chunge Qu[1]; Hongwei Tan[1]; Xuezhi Yin[2]; Xiufang Hu[1]

[1]University of Shanghai for Science and Technology, Shanghai, China.

[2]Shanghai Berry Electronic Technology Co., Ltd., Shanghai, China.

***Corresponding Author: Renling Zou**

University of Shanghai for Science and Technology, Shanghai, China.

Email: zourenling@163.com

Received: Mar 12, 2024

Accepted: Apr 15, 2024

Published: Apr 22, 2024

Archived: www.jcimcr.org

DOI: www.doi.org/10.52768/2766-7820/3000

Abstract

Symmetric structures are commonly used in various fields. To ensure the safety of these structures, it is crucial to employ appropriate damage detection methods. Among the methods used for structural health detection, the combination of structural dynamics and neural networks based on finite element models has gained popularity due to its non-destructive nature. This study presents a neural network-based damage detection approach for symmetrical structures, taking into account the similarity of modal features. By considering the interference of modal feature similarity, the proposed method effectively detects damage in symmetrical structures. In this approach, the rates of mode shape change before and after damage are used as inputs to the neural network, as they are found to be less sensitive to modeling errors compared to the mode shapes themselves. The effectiveness and adaptability of the method are validated through a numerical case analysis of a symmetrical load-bearing base plate used in walkers for patients with spinal cord injuries.

Keywords: Symmetry; Neural network; Damage detection; Finite element model; Modal features.

Introduction

Symmetry is an intrinsic property found in many natural and engineered structures. Symmetrical objects are not only aesthetically pleasing but also often the most optimal design choice for a structure. This is because asymmetry can introduce uneven loads or stresses [1]. As a result, symmetrical structures are widely used in various fields such as bridges, buildings, railways, and medical rehabilitation equipment. However, these structures are prone to unpredictable structural failures due to the different external loads they experience during their service life. Therefore, it is crucial to employ appropriate damage detection methods [2-4] to assess the structural health and ensure its safety. One popular non-destructive method for structural health detection is the combination of structural dynamics and neural networks based on finite element models [5]. Current research in the field focuses on two main aspects. The first aspect involves the utilization of different neural network models or the optimization of basic neural network models to compare their effectiveness in damage recognition. Wu et al. applied Back-Propagation (BP) neural network technology to identify the location of a simple three-layer frame and assess the degree of damage to individual components [6]. Similarly, Szewczyk and Hajela developed an improved BP neural network method for the inverse mapping between the stiffness of individual structural elements and global static displacements under test loads [7]. In another study, Elkordy et al. employed a BP neural network to identify a five-story building, with training samples obtained from a finite element model [8]. Chen et al. established a finite element model of the motor housing, compared the analysis results with experimental data, verified the

reliability of the finite element model, and proposed the use of genetic algorithms to optimize the neural network model [9]. Their findings demonstrated that the GA-BPNN model effectively predicts vibration characteristic signals derived from finite element models. Another approach explored by Teng et al. involved the use of a Convolutional Neural Network (CNN) to extract damage features of steel frame structures [10]. Their results indicated that the CNN neural network successfully detects both single and multiple damages in structures. Moreover, in 2020, Mousavi et al. introduced a Deep Convolutional Neural Network (DCNN) capable of learning features from original frequency data [11]. Additionally, Atha and Jahanshahi employed CNN to mitigate the interference of prior knowledge and human factors in metal surface corrosion damage assessment [12]. The second aspect focuses on changing the dynamic features of the neural network input to compare the effects of damage identification using different dynamic features such as natural frequency, mode shape, and other parameters. Researchers, like Guo et al., studied 6 marine jacket platforms and used the first-order mode shape and natural frequency as inputs to the neural network [13]. After training, the neural network achieved a prediction error of less than 8%. In the case of reinforced concrete beams, Bagheri et al. employed four identification methods based on frequency changes of modal parameters, Modal Assurance Criterion (MAC), Coordinate Modal Assurance Criterion (COMAC), and modal curvature [14]. They found that the modal curvature method most effectively describes beam damage.

Existing research has utilized structural symmetry to address various issues in damage identification [15-17]. In a similar vein, this paper proposes a neural networks-based approach for damage detection in symmetrical structures, taking into account the similarity of modal features. When conducting health checks on symmetrical structures, it is important to fully exploit their symmetry and focus on the modal feature similarity of their symmetric parts. This approach offers several advantages that are significant for the advancement of damage detection in symmetrical structures: (1) It is suitable for components with symmetry and has minimal impact on boundary conditions; (2) Considering symmetry can enhance the accuracy of damage detection, which is an important feature in many engineering structures; (3) This method simplifies the calculation scale and time as it only requires considering the symmetrical part of the component.

Methodology

Damage sensitive features

Efficient neural network-based damage detection using modal parameters requires careful selection of input data that is less susceptible to finite element model errors. This is crucial as the neural network's training patterns are derived from the finite element model. Inaccurate modeling can hinder accurate damage estimation if the modeling errors outweigh the modal sensitivity to damage. Lee et al. utilized natural frequencies and mode shapes as inputs for their neural network [18]. While natural frequencies provide more precise measurements, they are highly sensitive to environmental factors such as temperature. On the other hand, mode shapes are less affected by these environmental effects [19,20]. In real structures, the impact of temperature on natural frequencies can be greater than the effect of damage, posing challenges for damage detection.

This study explores the modal sensitivity based on the modal perturbation equation. The characteristic equation before and after structural damage without considering modeling errors is:

$$(K_u + \Delta K_d)(\varphi_u + \Delta\varphi_d) = (\lambda_u + \lambda_d)(\varphi_u + \Delta\varphi_d)M \quad (1)$$

Where K is the stiffness matrix, M is the mass matrix, λ is the square of the natural frequency, ϕ is the mode shape.

The subscripts u and d represent the intact and damaged conditions respectively. We assume that the mass change before and after structural damage is ignored and consider the structural modeling error. The characteristic equation related to the damage stiffness change ΔK_d is:

$$(K_u + \Delta K + \Delta K_d)(\varphi_u + \Delta\hat{\varphi} + \Delta\hat{\varphi}_d) = (\lambda_u + \Delta\hat{\lambda} + \Delta\hat{\lambda}_d)(\varphi_u + \Delta\hat{\varphi} + \Delta\hat{\varphi}_d)M \quad (2)$$

Where ^ represents the quantity related to the modeling error ΔK.

Assuming a small damage ΔK_d and a small damage modeling error ΔK, Δλ^ and Δλ^_d represent the changes in λ under the same damage ΔK_d for two finite element models, one without model error and one with model error. It can be approximated that $\Delta K_d = \Delta\hat{\lambda}_d$. In damage sensitive feature validation, a numerical verification of an example structure is provided. Additionally, the following formula is derived:

$$(K\_u-\lambda\_u\ M)\ (\Delta\varphi\_d-\Delta\hat{\varphi}\_d)=0 \quad (3)$$

The solution yields two situations:

$$(\Delta\varphi\_d-\Delta\hat{\varphi}\_d)=0 \quad (4)$$

$$\text{Or } (\Delta\varphi\_d-\Delta\hat{\varphi}\_d) =\alpha\ (\varphi\_u) \quad (5)$$

The Eq. (4) demonstrates that the modal shape changes caused by the same damage are identical in models with and without modeling errors. This suggests that the sensitivity of modal shape changes to modeling errors is lower compared to the modal shape itself. Eq. (5) reveals that the discrepancy in modal shape changes caused by the same damage in the model without modeling error is directly proportional to the mode shape in the model without modeling error. To investigate the existence of the non-zero proportionality constant α, both sides of Eq. (5) are multiplied by [ϕ_u] ^ T, resulting in the following equation:

$$\varphi_u{}^T(\Delta\varphi_d - \Delta\hat{\varphi}_d) = \alpha\varphi_u{}^T\varphi_u \quad (6)$$

Normalizing the mode shapes gives the following approximate relationship:

$$\varphi_u{}^T\Delta\varphi_d \approx 0, \varphi_u{}^T\Delta\hat{\varphi} \approx 0, \varphi_u{}^T\Delta\hat{\varphi}_d \approx 0 \quad (7)$$

The solution results indicate that Eq. (4) is the unique solution to Eq. (3). Assuming a small modeling error ΔK, the mode shape change rate before and after damage can be derived from the following approximate relationship based on Eq. (4):

$$\frac{\varphi_{dj}{}^i - \varphi_{uj}{}^i}{\varphi_{uj}{}^i} \approx \frac{\hat{\varphi}_{dj}^i - \hat{\varphi}_{uj}^i}{\hat{\varphi}_{uj}^i} \quad (8)$$

The rate of change of mode shape is less affected by modeling errors compared to the mode shape itself. Thus, the mode shape change rate is considered as the damage sensitive feature

and used as input for damage detection in the neural network.

Data extraction preprocessing

This study focuses on analyzing the symmetrical load-bearing base plate of a walking aid used by patients with Spinal Cord Injuries (SCI). The load-bearing base plate model is loaded into the MODAL module of ANSYS and divided into 16 modules based on the smallest symmetrical part, as depicted in Figure 1. Material values are assigned to different regions, and the degree of damage is simulated by adjusting the loss value of Young's modulus E. To analyze the modal behavior, the modal expansion number is set to 6th order for each damage condition. The load-bearing base plate is divided into meshes, and boundary conditions are added based on the actual connection conditions of the base plate. Modal vibration shapes are then obtained through calculations. The 6th-order mode shape of each damage condition is processed to determine the change rate. This change rate is normalized and used as the input data for the neural network.

Figure 1: Regional division of finite element model of symmetrical load-bearing plate

Neural networks for damage detection

In this study, a standard BP neural network was utilized for damage detection. The basic structure of its neurons is illustrated in Figure 2. The network comprises an input layer, a hidden layer, and an output layer, and the neuron layers are shown schematically in Figure 3.

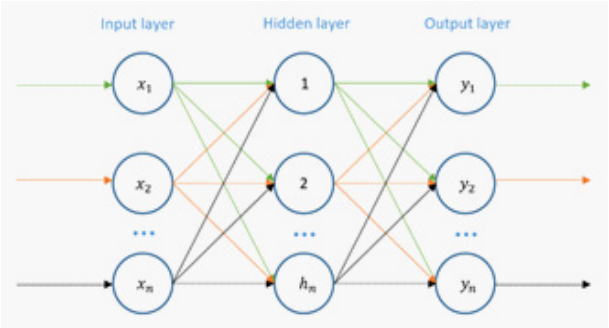

Figure 2: Schematic diagram of the basic structure of a neuron.

The rectified linear unit (Relu) activation function is used in the hidden layer and output layer. Its function is defined by Eq. 4, and the derivative of y with respect to x is given by Eq. 5.

In order to improve the performance of the fully connected layer, a Softmax layer is added. The function of the Softmax layer is defined as follows:

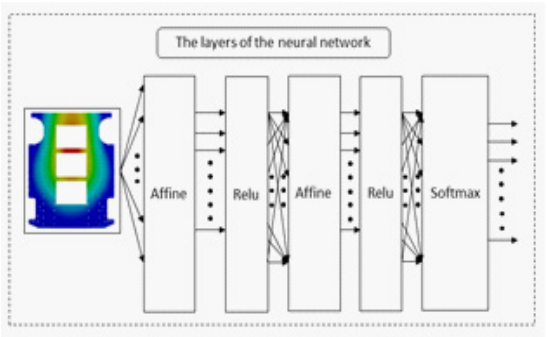

Figure 3: Schematic diagram of neuron layers.

$$y = \begin{cases} x, (x > 0) \\ 0, (x \leq 0) \end{cases} (9)$$

$$\frac{\partial y}{\partial x} = \begin{cases} 1, (x > 0) \\ 0, (x \leq 0) \end{cases} (10)$$

$$y_k = \frac{exp(a_i)}{\sum_{i=1}^{n} exp(a_i)} (11)$$

Where a_i represents the input signal and n is the number of neurons in the output layer.

Additionally, the Dropout method is employed to prevent overfitting. Furthermore, the ADAM gradient optimization algorithm is utilized to find the optimal parameters.

Damage detection overall plan

In this study, a model of a symmetrical load-bearing bottom plate for patients with SCI was used. The study aimed to explore the influence of modal feature similarity on symmetrical structures using a combination of structural dynamics and neural networks based on finite element models. The first step was to determine the damage sensitivity features and use the modal shape change rate as the input for the neural network, considering its higher sensitivity to damage compared to modeling error. The neural network model was then determined, with the BP neural network selected as the research tool for dynamic damage intelligent detection due to its popularity and evolution. The network consisted of an input layer, a hidden layer, and an output layer, with the Relu activation function used for the hidden and output layers. A Softmax layer was added after the fully connected layer, and the Dropout method was employed to suppress overfitting. The ADAM optimization algorithm was utilized to find the optimal parameters. The damage detection data was obtained from the finite element model. The symmetric load-bearing plate structure model was divided into 16 areas, and damage was simulated by changing the Young's modulus of each area. The Young's modulus loss value in each area ranged from 5% to 50% in steps of 5%, resulting in a total of 160*6 data samples for analysis of the first 6 mode shapes under each damage scenario. The acquired data were processed to obtain the modal shape change rate, which was then normalized and used as input for the neural network. The neural network learned to identify and classify injuries. The overall plan for damage detection of the load-bearing base plate structure is shown in Figure 4.

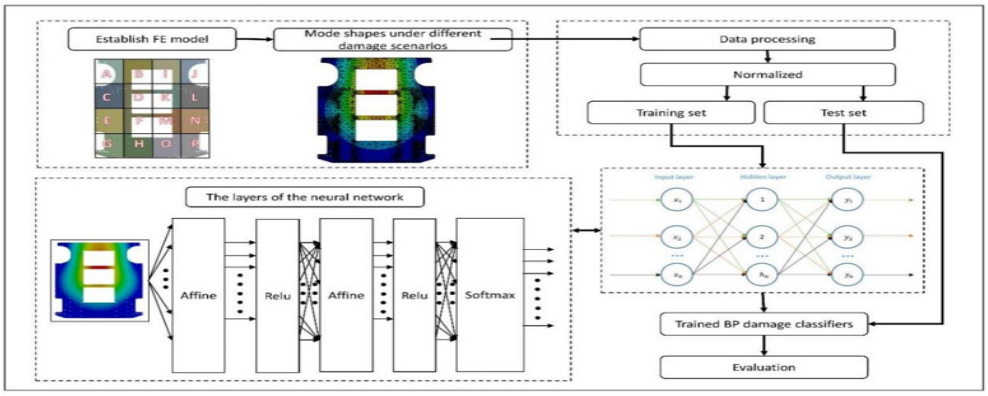

Figure 4: Overall scheme of structural damage detection.

Table 1: Injury scene simulation of symmetrical load-bearing boards of walkers in patients with spinal cord injury.

	Element regions															
	A	B	C	D	E	F	G	H	I	J	K	L	M	N	O	P
Case1+	—	—	—	—	—	10%	—	—	—	—	—	—	—	—	—	—
Case2	—	—	—	—	—	—	—	—	—	15%	—	—	—	—	—	—
Case3	—	10%	—	—	—	—	—	—	—	—	—	—	—	—	15%	—
Case4	—	—	—	—	15%	10%	—	—	—	—	—	—	—	—	—	—
Case5	10%	—	—	—	—	—	—	15%	—	—	—	—	10%	—	—	—
Case6	—	—	10%	—	—	—	—	—	15%	—	—	—	—	15%	—	—

+Case1: damage scenarios for 1th mode.

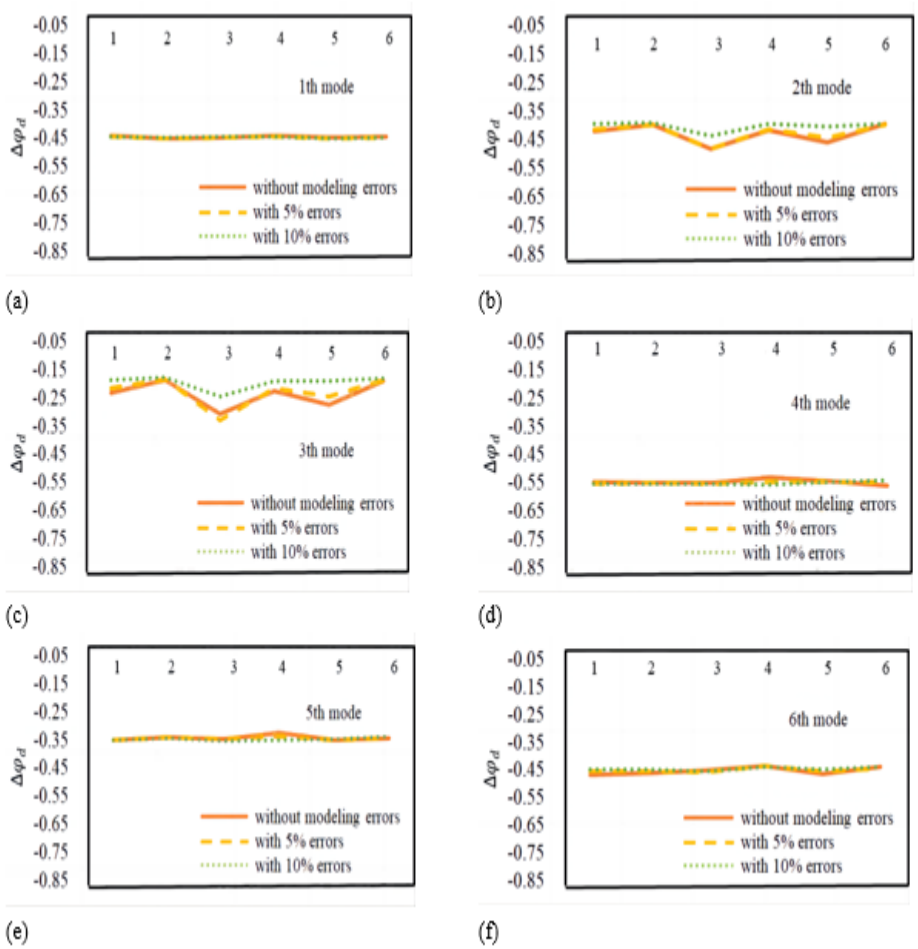

Figure 5: Numerical sensitive feature verification $\Delta\varphi_d \approx \Delta\hat{\varphi}_d$.

Numerical verification

Damage sensitive feature validation

To simulate the modeling error, the Young's modulus of the model was altered, and finite element models were created with no error, 5% error, and 10% error. Figure 1 illustrates the division of the load-bearing plate into 16 regions, where the Young's modulus of each region was adjusted to simulate the six damage scenarios mentioned in Table 1. The analysis provides the rate of change in the first six mode shapes of the finite element model under the six damage scenarios, considering both the presence and absence of modeling errors.

The results indicate that the rate of change in mode shape for the finite element model, both with and without modeling errors caused by structural damage, is nearly identical. This is depicted in Figure 5. Among the six damage cases analyzed, the average difference in mode shape change rate between the models with and without modeling errors is less than 0.58%.

Both theoretical and numerical simulation analyses have demonstrated that in the modal analysis of the finite element model, the sensitivity of the rate of change of mode shape to damage is higher than that to modeling error. Consequently, utilizing the modal shape change rate damage detection index as input for the neural network can mitigate the influence of modeling errors in the finite element model on the results of structural damage detection.

Symmetric structure modal similarity verification

Simulation case one

In the Case one, the training data is divided into two cases based on the modal feature similarity of symmetric structures. The selected area data in Method one contains geometric symmetry, while the selected area data in Method two does not contain geometric symmetry.

Method one: Figure 6(a) shows that the damage of the left half of the A, B, C, and D areas is set to label 0, and the damage of the E, F, G, and H areas is set to label 1. Similarly, the damage in the right half of the I, J, K, L regions is set to label 2, and the damage in the M, N, O, P regions is set to label 3. The training set is created by applying 60% of the 5%-50% damage modality parameters to all regions of A-P, while the remaining 40% is used as the testing set. The Young's modulus loss is varied from 5% to 50% in 5% steps for the 16 zones of the symmetrical load-bearing plate.

Method two: Figure 6(b) illustrates that the A-H region data of the left half of the geometric symmetry structure is selected as the training set. In this case, the damage of regions A and B is set as label 0, and the damage of regions C and D is set as label 1. Similarly, the damage in areas E and F is set as label 2, and the damage in areas G and H is set as label 3. On the other hand, the I-P data of the right half of the geometric symmetry structure is used as the test set. Here, the damage of regions I and J is set as label 0, the damage of regions K and L is set as label 1, the damage of regions M and N is set as label 2, and the damage of regions O and P is set as label 3.

The performance of Case one is evaluated using metrics such as Accuracy, Precision, Recall, F1 score, and Cohens kappa. The evaluation scores for Method one are as follows: Macro-accuracy 90%, Macro-F1 78.3%, and kappa 69.2%, as shown in Table 2. Similarly, the evaluation scores for Method Two are as follows:

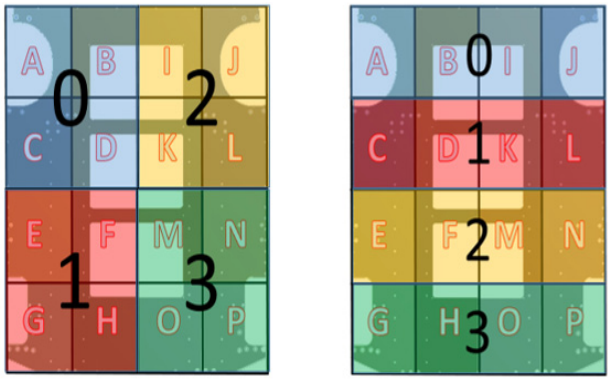

(a) Method one (b) Method two

Figure 6: Method one and two damaged area label assignment for simulation case one.

Macro-accuracy 99.5%, Macro-F1 98.9%, and kappa 97.2%, as shown in Table 3.

Table 2: Performance evaluation parameters of Method one for Simulation case one.

	Label 0	Label 1	Label 2	Label 3
Micro-accuracy	0.9	0.8	0.9	1
Precision	0.8	0.67	0.71	1
Recall	0.8	0.4	1	1
Micro-F1	0.8	0.5	0.83	1
Macro-accuracy	0.9			
Macro-F1	0.783			
kappa	0.692			

Table 3: Performance evaluation parameters of Method two for Simulation case one.

	Label 0	Label 1	Label 2	Label 3
Micro-accuracy	0.99	0.99	1	1
Precision	0.96	1	1	1
Recall	1	0.96	1	1
Micro-F1	0.9796	0.9796	1	1
Macro-accuracy	0.995			
Macro-F1	0.989			
kappa	0.972			

Analysis of the performance evaluation results reveals that Method two achieves significantly higher Macro-accuracy, Macro-F1, and kappa compared to Method one. Figure 7(a)-(b) illustrates the confusion matrix and accuracy of the classification results for Method one, while Figure 7c,7d illustrates the confusion matrix and accuracy of the classification results for Method two. In Method one, the classification accuracy for label 2 and label 3 is 100% each, followed by label 0 with 80%, and label 1 with the lowest classification accuracy of 40%. On the other hand, in Method two, the classification accuracy for labels 0, 2, and 3 is 100%, with only label 1 having a relatively lower classification accuracy of 96%. Evidently, Method one experiences misclassification due to the interference of similarity in modal features of symmetric structures. In contrast, Method two significantly improves the classification accuracy by excluding the interference of modal feature similarity in symmetric structures. Method two achieves this improvement by using the damage data from the left half of the symmetric structure as the training set and the damage data from the right half of the

symmetric structure as the test set, unlike Method one which uses 60% of the global damage data as the training set and 40% as the test set.

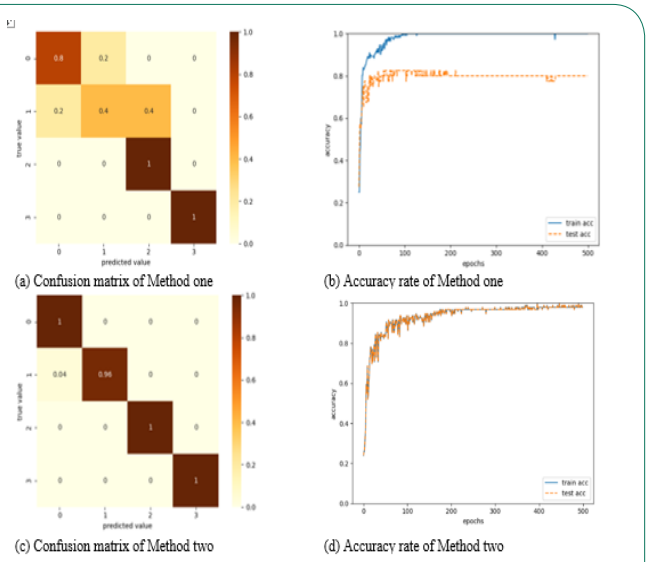

Figure 7: Confusion matrix and accuracy for Simulation case one.

Simulation case two

In the Case two, based on the analysis results of Numerical case one, the damage data of base plates C, D, E, and F with low recognition rates were selected for local damage recognition. The training data is divided into two cases to consider the modal feature similarity of similar structures.

Method one, the area data selected does not merge geometrically similar parts, as shown in Figure 8a. Areas C, D, E, and F of the symmetrical load-bearing plate are chosen for damage data, with assigned values of 0, 1, 3, and 2 respectively. The training set comprises 60% of the data, while the test set comprises 40%.

Method two merges the geometrically similar parts of areas D and E into a new area D, as depicted in Figure 8b. The damage data of areas C, D, and E are assigned values of 0, 1, and 2 respectively. The training set and test set are divided in the same proportions as in Method one.

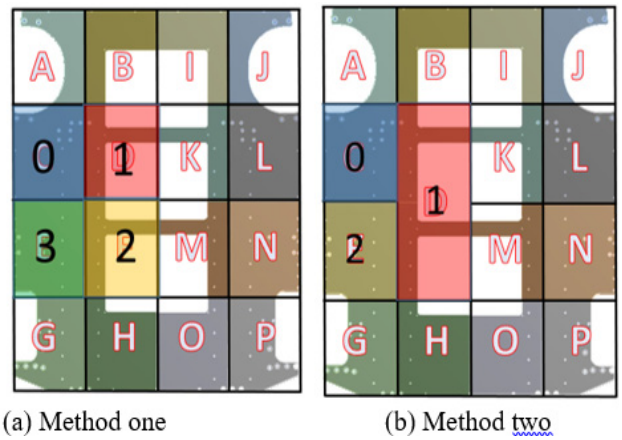

Figure 8: Method one and two damaged area label assignment for Simulation case two.

The evaluation scores for method one are as follows: Macro-accuracy 99.5%, Macro-F1 98.9%, and kappa 99.3%, as shown in Table 4. On the other hand, method two obtained the following scores: Macro-accuracy 100%, Macro-F1 100%, and kappa 100%, as shown in Table 5.

Table 4: Performance evaluation parameters of Method one for Simulation case two

	Label 0	Label 1	Label 2	Label 3
Micro-accuracy	1	0.98	1	1
Precision	1	1	1	1
Recall	1	0.92	1	1
Micro-F1	1	0.9582	1	1
Macro-accuracy	0.995			
Macro-F1	0.989			
kappa	0.993			

Table 5: Performance evaluation parameters of Method two for Simulation case two

	Label 0	Label 1	Label 2
Micro-accuracy	1	1	1
Precision	1	1	1
Recall	1	1	1
Micro-F1	1	1	1
Macro-accuracy	1		
Macro-F1	1		
kappa	1		

Analysis of the performance evaluation results reveals that method two significantly outperforms method one in terms of Macro-accuracy, Macro-F1, and kappa. Confusion matrices and accuracy of the classification results are depicted in Figure 9a,9b for method one and in Figure 9c,9d for method two. In case one, the classification accuracy for labels 0, 2, and 3 is 100%, while the accuracy for label 1 is 92%. In case two, the classification accuracy for labels 0, 1, and 2 all reaches 100%. It is evident that method one experiences misclassification due to the absence of exclusion of modal feature similarity interference among similar structures. Method two, on the other hand, improves the classification effect significantly by combining similar structures D and F into the same region and using 60% of the new global damage data of C, D, and F as the training set and 40% as the test set, thereby eliminating the interference of modal feature similarity.

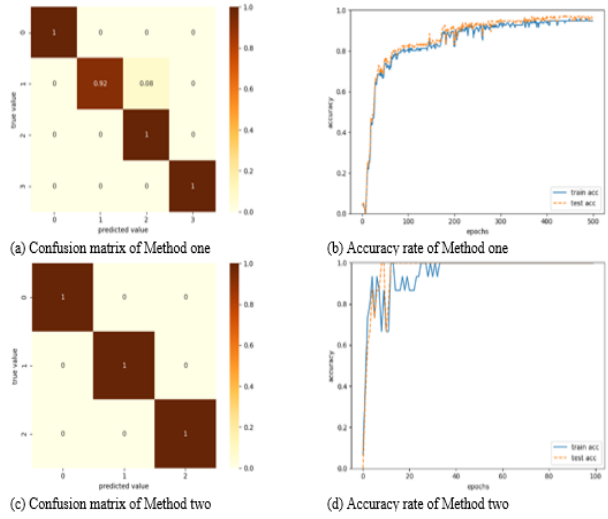

Figure 9: Confusion matrix and accuracy for simulation case two.

Conclusion

This study proposes a neural network-based method for damage detection in symmetrical structures, taking into account the similarity of modal features. The change rates of mode shapes are used as inputs to the neural networks, which helps to minimize the impact of modeling errors in finite element models and enables the construction of training data sets. To verify the effectiveness and adaptability of the proposed method, a numerical case analysis is performed on a symmetrical load-bearing base plate of a walker for patients with SCI. In simulation case one, half of the structural damage data in the symmetrical structure is selected as the training set to detect and classify the overall structural damage. This approach avoids the interference caused by the similarity of modal features in symmetrical structures, simplifies the analysis process, and significantly improves the accuracy of damage identification. Building upon this, simulation case two is conducted to study similar structures. Similar areas are merged into the same detection area to reduce interference from the similarity of modal features and further enhance the accuracy of damage detection.

Declarations

Acknowledgments: The authors would like to thank the Science and Technology Commission of Shanghai Municipality (grant number: 21S31906000) , the National Natural Science Foundation of China (NSFC) Grant 61803265 and Medical-industrial cross-project of USST Grant 1022308524 for founding the study.

Funding: This work was supported in part by Science and Technology Commission of Shanghai Municipality (grant number: 21S31906000) the National Natural Science Foundation of China (NSFC) Grant 61803265, in part by Medical-industrial cross-project of USST Grant 1022308524.

Competing interests: Authors state no conflict of interest.

References

1. Chen JG, Büyüköztürk O. A symmetry measure for damage detection with mode shapes. Journal of Sound and Vibration. 2017; 408: 123-137. https://doi.org/10.1016/j.jsv.2017.07.022.
2. Chase SB, Aktan AE. (2001). Health monitoring and management of civil infrastructure systems. Health Monitoring and Management of Civil Infrastructure Systems. 2001; 4337. https://doi.org/10.1533/9780857098986.2.141.
3. Doebling SW, Farrar CR, Prime MB. A summary review of vibration-based damage identification methods. Shock and vibration digest. 1998; 30(2): 91-105.
4. Zou Y, Tong LPSG, Steven GP. Vibration-based model-dependent damage (delamination) identification and health monitoring for composite structures-a review. Journal of Sound and vibration. 2000; 230(2): 357-378. https://doi.org/10.1006/jsvi.1999.2624.
5. Kudva JN, Munir N, Tan PW. (1992). Damage detection in smart structures using neural networks and finite-element analyses. Smart Materials and Structures. 1992; 1(2): 108. https://doi.org/10.1088/0964-1726/1/2/002.
6. Wu X, Ghaboussi J, Garrett Jr JH. Use of neural networks in detection of structural damage. Computers & structures. 1992; 42(4): 649-659. https://doi.org/10.1016/00457949(92)90132-J.
7. Szewczyk ZP, Hajela P. Damage detection in structures based on feature-sensitive neural networks. Journal of computing in civil engineering. 1994; 8(2): 163-178. https://doi.org/10.1061/(ASCE)0887-3801(1994)8:2(163).
8. Elkordy MF, Chang KC, Lee GC. Neural networks trained by analytically simulated damage states. Journal of Computing in Civil Engineering. 1993; 7(2): 130-145. https://doi.org/10.1061/(ASCE)0887-3801(1993)7:2(130).
9. Chen XY, Chen Z, Zhao Y. (2018). Numerical research on virtual reality of vibration characteristics of the motor based on GA-BPNN model. Neural Computing and Applications. 2018; 29: 1343-1355. https://doi.org/10.1155/2022/2976271.
10. Teng S, Chen G, Liu G, Lv J, Cui F. Modal strain energy-based structural damage detection using convolutional neural networks. Applied Sciences. 2019; 9(16): 3376. https://doi.org/10.1016/j.jsv.2016.10.043.
11. Mousavi Z, Varahram S, Ettefagh MM, Sadeghi MH, Razavi SN. (2021). Deep neural networks-based damage detection using vibration signals of finite element model and real intact state: An evaluation via a lab-scale offshore jacket structure. Structural Health Monitoring. 2021; 20(1): 379-405. https://doi.org/10.1177/1475921720932614.
12. Atha DJ, Jahanshahi MR. (2018). Evaluation of deep learning approaches based on convolutional neural networks for corrosion detection. Structural Health Monitoring. 2018; 17(5): 1110-1128. https://doi.org/10.1177/1475921717737051.
13. Guo B, Han J, Li X, Fang T, You A. (2016). Research and design of a new horizontal lower limb rehabilitation training robot. International Journal of Advanced Robotic Systems. 2016; 13(1): 10. https://doi.org/10.1177/1475921717737051.
14. Bagheri A, Alipour M, Ozbulut OE, Harris DK. A nondestructive method for load rating of bridges without structural properties and plans. Engineering Structures. 2018; 171: 545-556. https://doi.org/10.1016/j.engstruct.2018.05.114.
15. Drygala IJ, Dulinska JM. Full-scale experimental and numerical investigations on the modal parameters of a single-span steel-frame footbridge. Symmetry. 2019; 11(3): 404. https://doi.org/10.3390/sym11030404.
16. Yang Y, Yang L, Yao G. (2021). Post-processing of high formwork monitoring data based on the back propagation neural networks model and the autoregressive-moving-average model. Symmetry. 2021; 13(8): 1543. https://doi.org/10.3390/sym11030404.
17. Yao G, Sun Y, Wong M, Lv X. A real-time detection method for concrete surface cracks based on improved YOLOv4. Symmetry. 2021; 13(9): 1716. https://doi.org/10.3390/SYM13081543.
18. Lee J W, Kim JD, Yun CB, Yi JH, Shim JM. Health-monitoring method for bridges under ordinary traffic loadings. Journal of Sound and Vibration. 2002; 257(2): 247-264. https://doi.org/10.3390/sym13091716.
19. Farrar CR, James Iii GH. System identification from ambient vibration measurements on a bridge. Journal of sound and vibration. 1997; 205(1): 1-18. https://doi.org/10.1006/jsvi.1997.0977.
20. Ko JM, Chak KK, Wang JY, Ni YQ, Chan THT. Formulation of an uncertainty model relating modal parameters and environmental factors by using long-term monitoring data. In Smart Structures and Materials 2003: Smart Systems and Nondestructive Evaluation for Civil Infrastructures. 2003; 5057: 298-307. SPIE. https://doi.org/10.1177/1461348418786520.